Journal of Hazardous Materials 165 (2009) 704–713

Contents lists available at ScienceDirect

Journal of Hazardous Materials

journal homepage: www.elsevier.com/locate/jhazmat

Interactions of NO_2 with activated carbons modified with cerium, lanthanum and sodium chlorides

Karifala Kante, Eleni Deliyanni [1], Teresa J. Bandosz *

Department of Chemistry, The City College of New York The Graduate School of the City University of New York, 138 St. Convent Avenue, New York, NY 10031, USA

ARTICLE INFO

Article history:
Received 28 May 2008
Received in revised form 6 October 2008
Accepted 12 October 2008
Available online 5 November 2008

Keywords:
Activated carbons
Adsorption
Nitrogen dioxide
Oxidation

ABSTRACT

Highly porous wood-based activated carbon was impregnated with cerium, lanthanum and sodium chlorides using incipient impregnation method. On the samples prepared adsorption of NO_2 was carried out from moist (70% humidity) air either with or without the prehumidification. The materials were characterized using adsorption of nitrogen, thermal analysis, FTIR, and potentiometric titration. The results indicated that for all materials a significant amount of NO_2 was reduced to NO and released from the system. In the case of virgin carbons, the NO_2 interacting with the surface along with nitric and nitrous acids formed there in the presence of water significantly increased the acidity of the carbons by the formation of oxygen-containing groups and organic nitrates. On the other hand, when chlorides were present the capacity to interact with nitrogen dioxide increased since the inorganic phase, depending on the nature of metal, bound NO_2 in the forms of nitrates (Ce, La, Na), got oxidized/oxidized carbon surface (for Ce) or contributed to the formation of nitrosyl chloride (for Na).

1. Introduction

Nitrogen dioxide, besides being a toxic industrial gas, is also considered as a main air pollutant contributing to the formation of photochemical smog and acid rain [1]. Its main source in the environment is from photochemical oxidation of NO released from power plants and car engines during fossil fuel burning. NO_2 and NO are often referred to as NO_x. Since their presence in the atmosphere also affects human health [2] the efforts continue towards controlling and minimization the emissions of those gases.

Adsorption and reduction of NO_2 at conditions close to ambient have been studied extensively on various adsorbents including carbonaceous materials such as activated carbon fibers [3], soot [4,5], carbon black [5,6], char [7], carbon nanotubes [8], and activated carbon [2,9–12]. Application of activated carbons for adsorption/reduction of NO_2 is driven by their developed pore structure [13–16]. Nevertheless, surface chemistry represented by the type, number and chemical arrangement of heteroatoms on their surface is also considered as important. Those heteroatoms exist in the forms of functional groups and are located at the edges of the graphene layers. It was shown that this aspect of surface heterogeneity affects adsorption, electrochemical, catalytic, acid–base, redox, hydrophilic or hydrophobic character and other properties of activated carbons [17–19].

As indicated in the literature, as a result of NO_2 interactions with the carbon surface in the presence of oxygen and water at ambient temperatures various surface complexes are formed such as C–NO_2, C–ONO, C–ONO_2, and C–O [2,9–11,20]. Those surface complexes, existing mainly on the outer surface can be considered as temporary entities leading to further chemical transformations or as new functional groups, depending on their stability and environmental conditions. To increase the adsorption efficiency via surface reactions, carbon can be impregnated with various species such as KOH [21,22], which react with NO_2 forming nitrates, or transition metals, such as copper, on which reduction could occur [10,12,23–25]. These kinds of modifications follow the studies on inorganic materials, as, for example, on alumina, KOH impregnated alumina, MgO, Fe_2O_3 or TiO_2, which showed that chemisorption via nitrite and nitrate formation is the main adsorption/reactive adsorption mechanism on their surfaces [26].

The objective of this paper is to investigate the effects of deposition of cerium(III), lanthanum(III), and sodium chlorides on the activated carbon surfaces on the adsorption and reduction of NO_2 at ambient conditions. These compounds were chosen based on their reactivity with nitrogen dioxide via oxidation/reduction reactions and formation of nitrates. The performance is analyzed taking into account the effects of surface chemistry and porosity on the

* Corresponding author. Tel.: +1 212 650 6017; fax: +1 212 650 6107.
E-mail address: tbandosz@ccny.cuny.edu (T.J. Bandosz).
[1] Permanent address: Section of Chemical Technology & Industrial Chemistry, School of Chemistry, Aristotle University, Box 116, GR-54124 Thessaloniki, Greece.

0304-3894/$ – see front matter © 2008 Elsevier B.V. All rights reserved.
doi:10.1016/j.jhazmat.2008.10.092

conversion of NO_2, and its interactions with both, a carbon surface and an inorganic phase.

2. Experimental

2.1. Materials

Wood-based activated carbon BAX-1500 manufactured by Mead Westvaco was used in this study. The initial sample is designated as B. Modification via incipient impregnation [27] was performed and the concentration of chlorides was chosen to result in the deposition of 0.7 mmoles of either sodium, cerium(III) or lanthanum(III), depending on the surface treatment. This results in deposition of 2.3, 10, and 10 wt.% sodium, cerium and lanthanum, respectively. After impregnation, the carbon samples were air dried to constant mass. Although the excess of water was removed, the water associated with the hydration of chloride was expected to be still present in the system. The samples are designated as B-Na, B-Ce and B-La according to the metal chloride used for impregnation.

The samples after NO_2 adsorption were washed in a Soxhlet apparatus to remove water-soluble compounds/salts present on the surface in order to evaluate the changes in the chemistry of carbon matrix. They are designated with letter W following their names, as, for example, B-NaW.

2.2. Methods

2.2.1. NO_2 breakthrough capacity

The home designed dynamic test was used to evaluate NO_2 adsorption from gas streams [12]. Samples (1–2 mm particle size) were packed into a glass column (length 370 mm, internal diameter 9 mm, bed volume 3 cm^3). Dry or moist air (70% humidity) with 0.1 wt.% of NO_2 (accelerated test) was passed through the column of adsorbent at 0.450 L/min for NO_2. The sample were either prehumidified over night with moist air (70%) or used as received. The residence time was 0.4 s which is in the range of that used in industrial air filtration systems [28]. The flow rate was controlled using Cole Parmer flow meters. The breakthrough of NO_2 and the concentration of NO were monitored using MultiRAE Plus PGM-50/5P with electrochemical sensors. The tests were stopped at the breakthrough concentration of 20 ppm. The interaction capacities of each sorbent in terms of mg of NO_2 per g of adsorbent were calculated by integration of the area above the breakthrough curves, and from the NO_2 concentration in the inlet gas, flow rate, breakthrough time, and mass of sorbent [12]. The samples run in dry air, moist air, and after prehumidification are designated with the letters ED, EM, and EP, respectively.

2.2.2. Surface pH

A 0.4-g sample of dry carbon powder was added to 20 ml of distilled water and the suspension was stirred overnight to reach equilibrium. Then the pH of suspension was measured.

2.2.3. Thermal analysis

Thermal analysis was carried out using a TA Instruments Thermal Analyzer. The instrument settings were: heating rate, 10 °C/min and a nitrogen atmosphere at 100 mL/min flow rate. For each measurement about 30 mg of a ground adsorbent were used.

2.2.4. Potentiometric titration

Potentiometric titration measurements were performed with a DMS Titrino 716 automatic titrator (Metrohm). The instrument was set at the mode when the equilibrium pH was collected. Subsamples of the materials studied of about 0.100 g in 50 mL 0.01 M $NaNO_3$ were placed in a container thermostatted at 298 K and equilibrated overnight with the electrolyte solution. To eliminate the influence of atmospheric CO_2, the suspension was continuously saturated with N_2. The carbon suspension was stirred throughout the measurements. Volumetric standard NaOH (0.1 M) was used as the titrant. The experiments were done in the pH range of 3–10. Each sample was titrated with base after acidifying the sample suspension.

The surface properties were evaluated first using potentiometric titration experiments [29,30]. Here, it is assumed that the population of sites can be described by a continuous pK_a distribution, $f(pK_a)$. The experimental data can be transformed into a proton binding isotherm, Q, representing the total amount of protonated sites, which is related to the pK_a distribution by the following integral equation:

$$Q(\mathrm{pH}) = \int_{-\infty}^{\infty} q(\mathrm{pH}, pK_a)\, f(pK_a)\, \mathrm{d}pK_a \quad (1)$$

The solution of this equation is obtained using the numerical procedure [29,30], which applies regularization combined with non-negativity constraints. Based on the spectrum of acidity constants and the history of the samples, the detailed surface chemistry was evaluated. This kind of evaluation is valid only for samples on whose surface the chemical reaction/dissolution does not take place [29,30].

2.2.5. Evaluation of porosity

Nitrogen isotherms were measured at −196 °C using an ASAP 2010 (Micromeritics). Prior to each measurement, all samples were outgassed at 120 °C for the initial samples and 100 °C for the exhausted ones to avoid extensive decomposition of ammonia containing compounds. Approximately 0.20–0.25 g of sample was used for these analyses. The surface area, S_{BET}, (BET method), the micropore volume, V_{mic}, (Dubinin–Radushkevitch method, D–R) [31], the mesopore volume, V_{mes}, the total pore volume, V_t, were calculated from the isotherms. The pore size distributions (PSDs) were obtained using DFT method, which is described elsewhere [32,33].

2.2.6. FTIR

Fourier transform infrared (FTIR) spectroscopy was carried out using a Nicolet 380 FT-IR spectrometer using the smart diffuse reflectance method. 2–3 wt.% powdered samples were added to 97–98 wt.% of KBr matrix for measurement. The spectra were then collected within the range of 4000–400 cm^{-1}, 96 times at a resolution of 4 cm^{-1} to reduce the background noise. To measure the background spectrum pure KBr was used.

3. Results and discussion

The NO_2 breakthrough curves measured at different conditions on our materials are presented in Fig. 1. Striking difference is in the shape of the curves. With an increase in the amount of water accumulated in the system (supplied with the air stream) the curves reach their maximum, then the concentration of NO_2 emitted decreases, sometimes to zero, to increase again to 20 ppm which is the limit of our sensor. Then, when the adsorbents are purged with air the concentration of NO_2 rapidly decreases indicating the strong retention on the surface. On the other hand, concentration of NO reaches the sensor limit of 100 ppm after few minutes in each case and thus cannot be further monitored.

The breakthrough capacities calculated from the breakthrough curves are collected in Table 1 along with the surface pH val-

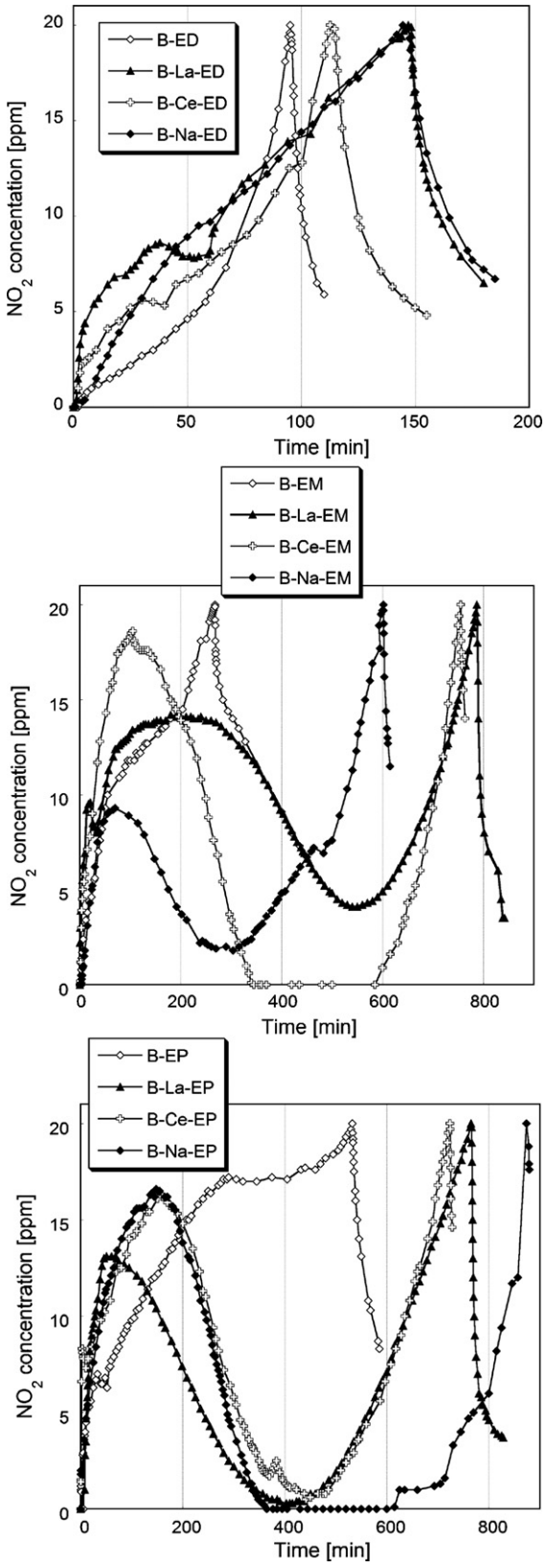

Fig. 1. NO_2 breakthrough curves.

Table 1
NO_2 breakthrough capacity, water preadsorbed and the surface pH values before and after NO_2 adsorption.

Samples	Adsorption capacity (mg/g)	Water preadsorbed (mg/g)	pH
B			5.84
B-W			5.57
B-ED	39		2.15
B-EM	64		2.07
B-EP	87	1099	1.83
B-EP-W			3.50
B-La			2.73
B-La-ED	17		2.08
B-La-EM	108		1.86
B-La-EP	143	284	1.65
B-La-EP-W			3.35
B-Ce			2.97
B-Ce-ED	29		1.96
B-Ce-EM	215		1.69
B-Ce-EP	184	831	1.69
B-Ce-EP-W			3.46
B-Na			5.30
B-Na-ED	30		1.83
B-Na-EM	198		2.66
B-Na-EP	283	861	1.53
B-Na-EP-W			3.57

ues and the amounts of water adsorbed during prehumidification. Generally, as seen from the breakthrough curves, the presence of water increases the capacity, especially when the sufficient amount of water is preadsorbed on the surface. That increase is 7–8-folds in comparison to the experiments run in dry conditions. Moreover, metal chlorides increase performance about 3-folds in comparison with the virgin carbons. The extent of that increase depends on the kind of metal used. Overall it looks like the impregnation with sodium chloride is the most efficient and with lanthanum chloride-the least efficient one. When the experiments are run in dry conditions, the performances of sodium and cerium chloride impregnated carbons are comparable.

Impregnation with chlorides, which can be considered as Lewis acids, significantly decreases the surface pH of carbon. Then after NO_2 exposure the surface became even more acidic, especially in the case of sodium modified material. For this carbon the drop in the pH was the most pronounced, almost four units, whereas for cerium and lanthanum that decrease is only one pH unit. If we assume that: (1) the amounts of NO_2 adsorbed have a direct effect on the amount of acid formed on the surface [34], and (2) those amounts are of similar orders of magnitudes, the changes in the pH suggest that in the case of B-Ce and B-La stronger acids are formed than in the case of B-Na. As expected, the surface pH decreases also for the virgin carbon as a result of formation of nitrogen-containing acids and oxidation of the carbon surface [19,33].

To hypothesize about the mechanism of NO_2 interactions with the surface of our carbons their texture and surface chemistry before and after exposure to NO_2 should be analyzed ad discussed. The parameters of pore structure calculated from adsorption of nitrogen are collected in Table 2. Impregnation resulted in a significant decrease in the structural parameters, especially in the case of cerium and lanthanum chloride-modified carbons. In those materials about 10 wt.% metals was introduced to the surface, which certainly contributes to “dilution effects” in structural parameters (decrease) via the addition of nonporous matter. Moreover, those chlorides are expected to be deposited in the pore system decreasing the pore volume. Their effect is especially seen as a marked

Table 2
Parameters of the porous structure calculated from nitrogen adsorption isotherms.

Sample	S_{BET} (m^2/g)	V_t (cm^3/g)	V_{meso} (cm^3/g)	V_{mic} (cm^3/g)	V_{mic}/V_t (%)
B	2143	1.494	0.696	0.798	53
B-W	2131	1.488	0.665	0.823	55
B-ED	1866	1.306	0.613	0.693	53
B-EM	1531	1.032	0.438	0.594	58
B-EP	1454	0.975	0.417	0.558	57
B-EP-W	1972	1.350	0.599	0.751	56
B-La	1574	1.075	0.584	0.491	54
B-La-ED	1260	0.861	0.384	0.477	55
B-La-EM	925	0.579	0.189	0.390	67
B-La-EP	686	0.405	0.112	0.293	72
B-La-EP-W	849	0.484	0.106	0.378	78
B-Ce	1502	1.043	0.488	0.555	53
B-Ce-ED	1496	1.040	0.496	0.544	52
B-Ce-EM	944	0.614	0.232	0.382	62
B-Ce-EP	950	0.612	0.230	0.382	62
B-Ce-EP-W	1740	1.185	0.529	0.656	55
B-Na	1952	1.372	0.626	0.746	54
B-Na-ED	1637	1.150	0.543	0.607	53
B-Na-EM	1306	0.862	0.350	0.512	59
B-Na-EP	1263	0.809	0.307	0.502	62
B-Na-EP-W	1829	1.255	0.555	0.700	56

decrease in the volume of mesopores. In the case of B-Na only about 2 wt.% sodium is introduced and thus a NaCl effect on the overall porosity is much smaller than in the case of other two chlorides.

After exposure to NO_2 in moist conditions accompanied by an increase in the content of water, the surface areas gradually decrease and the lowest is measured for B-La-EP. For this carbon 80% the original mesopore volume is not accessible for nitrogen molecules. For other carbons the extent of this effect reaches 50%. That decrease is less pronounced for virgin carbon. The small adsorption capacity can contribute to this effect. It is interesting that for all samples the volumes in pores smaller than 10 Å increase after exposure to NO_2, which can be linked to an oxidative effect of nitrogen dioxide and acids formed from nitrogen oxides on the surface of carbons. That volume even further increased after washing of the EP samples as a result of the removal of adsorbed oxidation products. After washing, although the surface of all samples increased, the original values measured for non-impregnated carbon were not reached, which suggests the changes in the texture caused by oxidation. In the case of B-LaEP-W only a slight increase in the porosity was noticed compared to the unwashed counterparts, which indicates that species insoluble in water (chlorides, nitrates and nitrites are soluble) are formed on the surface of this carbon and their chemical nature significantly differs from the chemical nature of the salts present on the surfaces of the B-NaEP and B-CeEP samples.

More details on porosity and trends in their changes are seen in Fig. 2 where pore size distributions (PSDs) are compared. Although the smallest changes, as expected, are seen in the case of virgin carbon, the trends observed for all samples but the sample modified with lanthanum, are similar. For the B-La mesopores with sizes between 20 and 100 Å are affected to greatest extent and washing does not remove the deposit from the carbon surface.

Although porosity is important to provide a contact of an adsorbate with the carbon surface and space for the hypothetical deposition of surface reaction products, without a proper surface chemistry the transformations of NO_2, which ensure its strong retention on the surface, are not expected to occur. The FTIR spectra for the carbons studied are presented in Figs. 3 and 4. The bands at about 1020–1220 cm^{-1}, 1665–1760 cm^{-1} and 2500–3300 cm^{-1} represent carboxylic groups incorporated to the carbon surface. The bands 1160–1200 cm^{-1} and 2500–3620 cm^{-1} (O–H band/stretch) are assigned to phenolic groups. On the exhausted samples, new bands appear at 1430 cm^{-1}, which represent to the presence of nitrogen as nitrates (NO_3^-) [35–41]. The intensity of that band is associated with the band at about 820 cm^{-1}, which also represents nitrates. An increase in the intensity of the band at about 1100 and 1600 cm^{-1} is also seen which suggests an increase in the number of carboxylic acid functional groups as a result of carbon surface oxidation. The well pronounced band at about 1550 cm^{-1} observed for the exhausted samples can be linked to incorporation of nitrogen as $-NO_2$ structures attached either to aromatic rings or aliphatic groups at the edges of graphene layers. This is in agreement with the hypothesized presence of nitric acid on the surface, demonstrated by the low pH values and the well known oxidative effect of that acid on the carbon surface. It is interesting that the band at about 1430 cm^{-1} is not so pronounced for the cerium containing carbon as for the other materials studied, which suggests less nitric acid/nitrates are present on its surface. After washing, the spectra for all carbons look similar indicating an increase in the number of oxygen containing groups and $-NO_2$ entities incorporated to the carbon structure. The visible feature seen on B-La spectrum after exposure to NO_2, which in fact differentiates this sample from the others, is an increase in the intensity of the band at about 1150 cm^{-1}. It may be linked to the presence of species, likely salts, which seem to be water insoluble since they were not removed during extensive washing.

The effects of NO_2 exposure on the carbon matrix chemistry are also seen on the proton binding curves (Fig. 5) and the calculated from them the distributions of pK_a of the species present on the surface of our carbons after washing (Fig. 6). Only initial and washed samples were studied. We limited the number of samples analyzed since any reaction/dissolution occurring on the surface due to the presence of an inorganic phase could lead to false results [30]. Once again, while the virgin carbon and those modified with sodium and cerium look similar and show an increase in the acidity compared to their non-exposed to NO_2, counterparts, the curve for the lanthanum modified sample shows a continuous proton release which can be associated with the reactions/dissolution of an inorganic phase present on this carbon and not removed

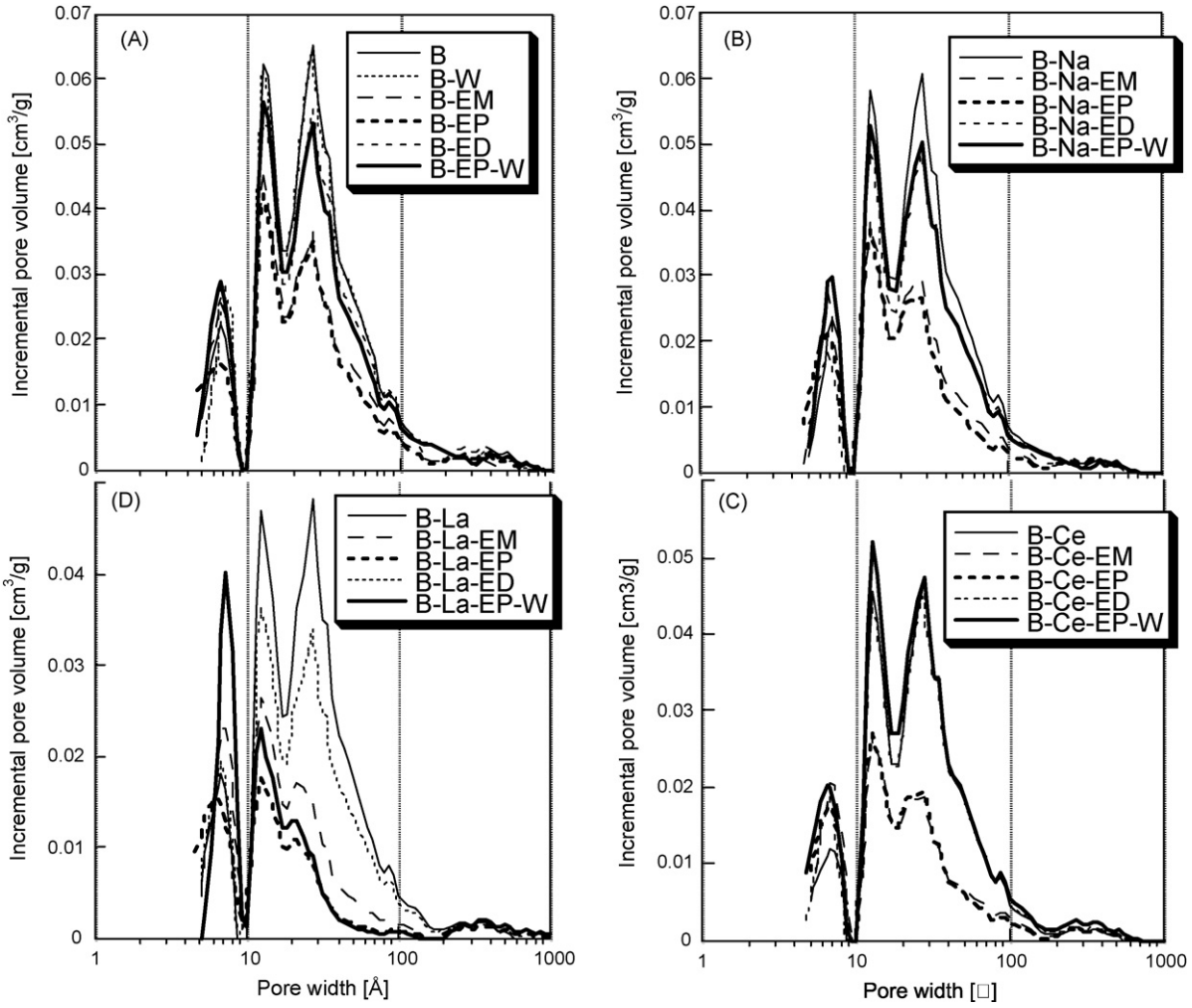

Fig. 2. Pore size distributions for the series of virgin carbon (A), B-Na (B), B-Ca (C), and B-La (D).

by NaOH added to the system during titration. This is in agreement with the differences observed in the FTIR spectra. For other carbons, consistent with the FTIR results, an increase in the number of all groups is found, especially those with pK_a greater than 6. The pK_a distribution for B-LaEP-W is not shown due to that assumption, discussed above, that the results are rather affected by chemical reactions (formation of water soluble species during titration) than adsorption and desorption of protons. As seen from Table 3 the most acidic carbon matrix and thus that one where the product of surface reactions had the greatest oxidation capability is the sample modified with cerium. Virgin carbon and its sodium-modified counterpart resemble each other. Their distribution patterns are similar to that obtained for the surface of BAX carbon exposed to nitric acid oxidation [40]. This once again suggests different surface reaction mechanisms for all three samples studied.

The changes in the surface of our carbons upon exposure to NO_2 and water washing can be also seen on DTG curves presented in Figs. 7 and 8. One has to remember that BAX carbon is manufactured at about 600 °C so it is not appropriate to interpret changes in DTG curves at temperatures higher than that. The first peak represents the removal of physically adsorbed water and nitric/nitrous acid and the decomposition of nitrates [39]. Then the curves become much more complex at temperature between 200 and 1000 °C. It is difficult to analyze them quantitatively since the species desorbed as the first peak contribute significantly to the total mass of the sample studied. Nevertheless, it is clearly seen than even if we analyze the pattern only up to 600 °C two distinguished groups of peaks can be noticed between 200 and 350 °C and between 350 and 450 °C. While the latter is more pronounced for virgin carbon and its sodium counterpart, the former is much more intense for the cerium and lanthanum modified samples. Taking into account the narrow temperature range and the decomposition temperature of cerium and lanthanum nitrates [39] we assign the peak between 200 and 300 °C to those species. The other peaks, at higher temperatures, especially those present after washing and thus removal of inorganic water-soluble salts, represent decomposition of functional groups formed as a results of the exposure to NO_2 [41]. Detailed discussion on the thermal decomposition of species present on the surface of carbonaceous materials (soot) after reaction with NO_2 was presented by Mckenhuber and Grother [42]. According to them reaction between NO_2 an soot at room temperature results in oxidation of carbon and formation of such oxygen containing functional groups as carboxylic acids (which decompose at 140 °C), lactones (few configurations; decomposing between 200 and 600 °C), carboxylic anhydrides (decomposing at 675 and 740 °C), and carbonyls, ether and quinines (decomposing at 750 °C). The peak on the sodium-modified sample at about 900 °C represents reduction of sodium by carbon [42].

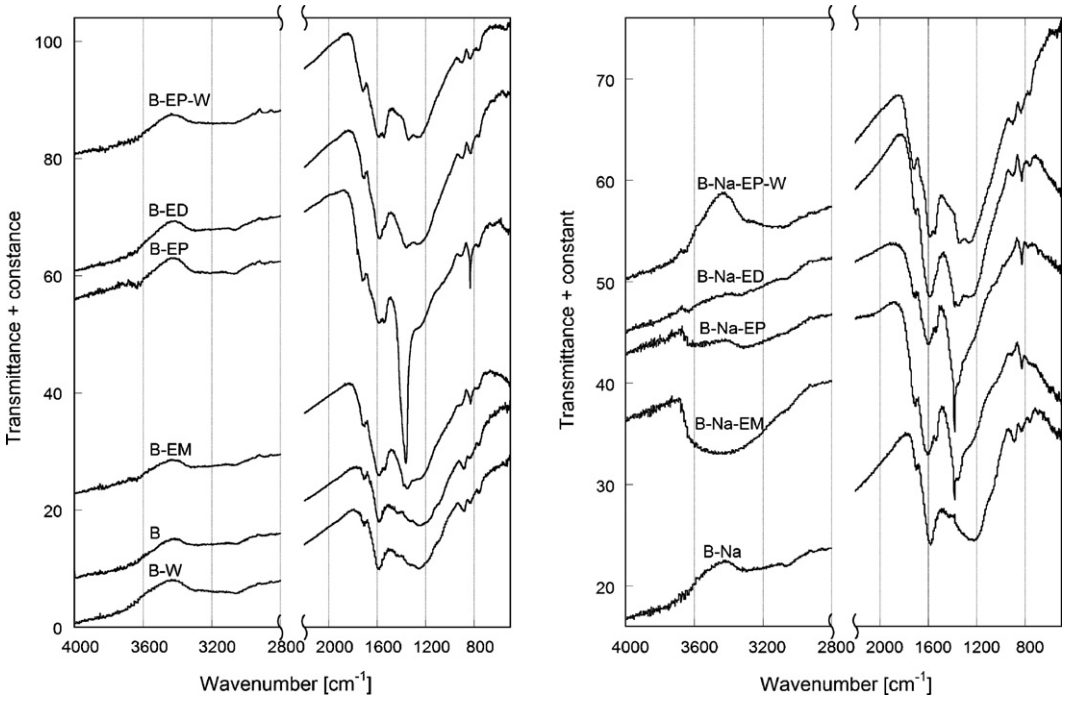

Fig. 3. FTIR spectra for virgin carbon and B-Na series of samples.

Taking into account the shapes of the breakthrough curves measured in the presence of water, the mechanism of NO_2 reactions on the surface apparently changes with time. This indicates that the formation of one product likely affects the reaction path. Even in the case of virgin carbon, without any metals, the slope changes. According to Jequirim et al. [34] the following reactions likely occur on the carbon phase in dry conditions, which explains formation of NO and then NO_2 breakthrough when all active sites for reaction/adsorption are saturated:

$$-C* + NO_2 \rightarrow C(O) + NO \quad (2)$$

$$-C(O) + NO_2 \rightarrow -C(ONO_2) \quad (3)$$

$$-C-C(ONO_2) \rightarrow CO_2 + NO + -C* \quad (4)$$

$$-C-C(ONO_2) \rightarrow CO + NO_2 + -C* \quad (5)$$

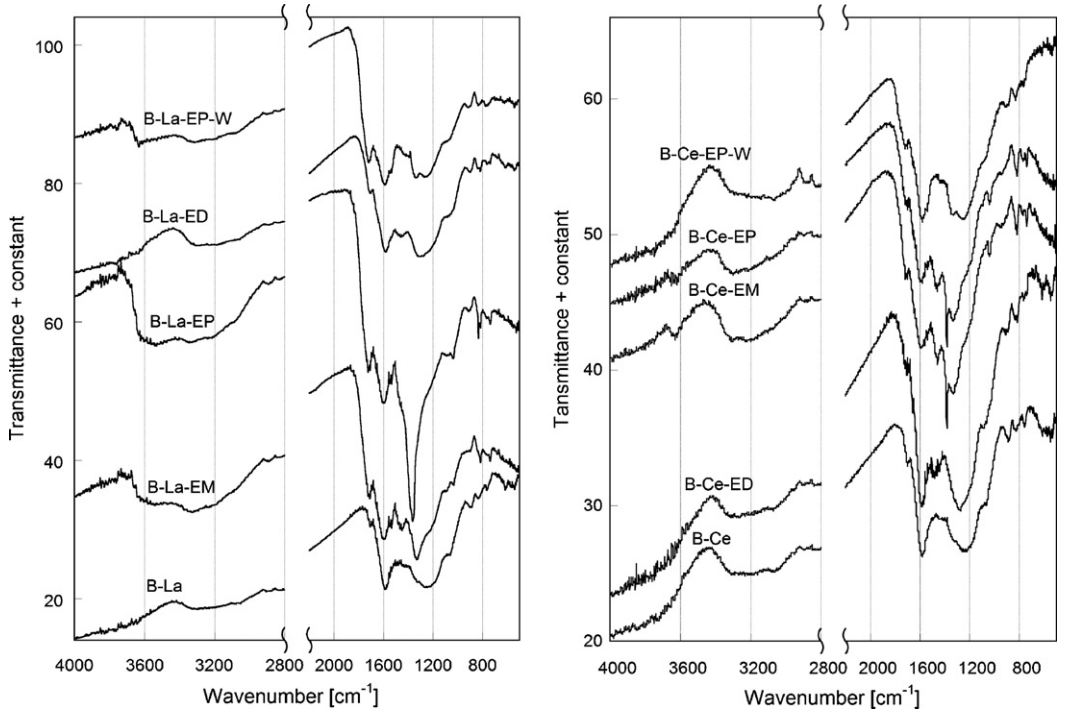

Fig. 4. FTIR spectra for B-La and B-Ce series of samples.

Table 3
pK_a values and the number of species represented by those pK_as (mmol/g).

Samples	p*K* 3–4	p*K* 4–5	p*K* 5–6	p*K* 6–7	p*K* 7–8	p*K* 8–9	p*K* 9–10	p*K* 10–11	All
B		4.53 (0.097)	5.77 (0.060)	6.87 (0.114)	7.55 (0.052)	8.43 (0.059)	9.61 (0.137)	11.1 (0.319)	(0.838)
B-W		4.03–4.88 (0.066–0.053)		6.05–6.75 (0.065–0.057)		8.99 (0.094)		10.13 (0.209)	(0.544)
B-EP-W		4.05 (0.149)	5.03 (0.137)	6.08–6.89 (0.148–0.159)	7.8 (0.038)	8.11–8.98 (0.148–0.159)		10.13 (0.315)	(1.253)
B-La-EP-W	3.29 (0.103)	4.09–4.72 (0.126–0.172)	5.58 (0.264)	6.49 (0.165)	7.21 (0.205)	8.40 (0.260)	9.72 (0.326)	10.14 (0.125)	(1.746)
B-Ce-EP-W		4.32 (0.265)	5.57 (0.235)	6.44 (0.137)	7.10 (0.175)	8.08 (0157)	9.02 (0.231)	10.18 (0.408)	(1.608)
B-Na-EP-W		4.63 (0.174)	5.68 (0.055)	6.42 (0.208)	7.68 (0.060)	8.74 (0.216)		10.22 (0.385)	(1.098)

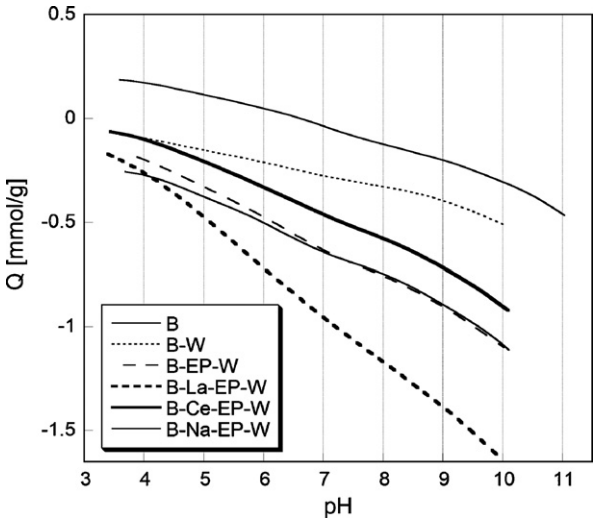

Fig. 5. Proton binding curves for the initial and exhausted carbons after washing.

where –C* represents a carbon active site and –C(O)–carbon oxygen complexes. Those oxygen complexes should include also oxygen engaged in functional groups.

In the overall, oxidation reaction of the carbon surface occurs:

$$C + 2NO_2 \rightarrow CO_2 + 2NO \quad (6)$$

$$C + NO_2 \rightarrow CO + NO \quad (7)$$

Binding of NO_2 to the surface as a first step of surface reaction a room temperature was also proposed by Muckenhuber and Grothe [42]. According to them more complex reaction occur at higher temperatures when oxygen containing functional group can be involved. The complexity of those arenas–NO_2 interactions on model compounds was also studied by Ghingo et al., who concluded that direct nitration does not take place at room temperature [43].

In wet conditions nitric acid and carbonic acids can be formed as separate phases [34]:

$$3NO_2 + H_2O \rightarrow 2HNO_3 + NO \quad (8)$$

$$CO_2 + H_2O \rightarrow 2H_2CO_3 \quad (9)$$

This nitric acid has even greater effect on oxidation of the carbon surface and the reaction of NO_2 with water certainly increases the

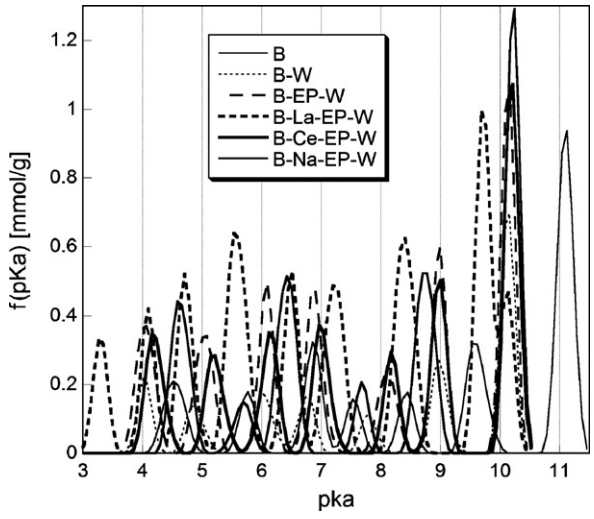

Fig. 6. pK_a distributions for the initial carbon and exhausted carbons after washing.

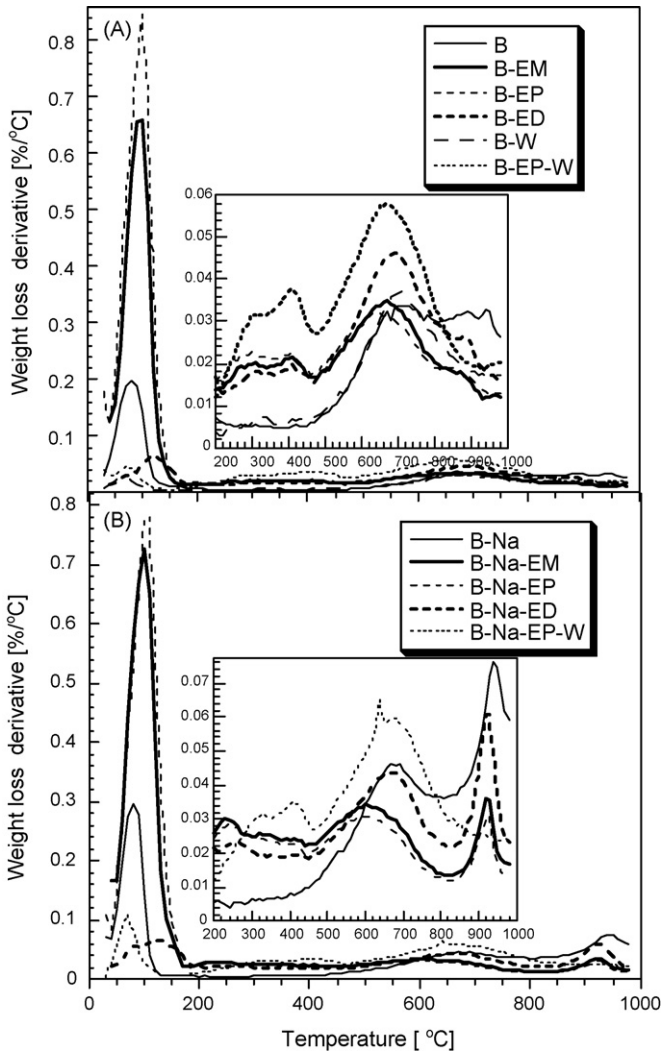

Fig. 7. DTG curves for the virgin carbons (A) and B-Na (B) series of carbons.

amount of NO_2 retained on the surface [12,22]. That water, owing to slow kinetics [44], needs some time to be adsorbed. This can explain the observed increase in the breakthrough time when the virgin carbon is prehumidified overnight. When the metals are present in the form of chlorides at least two mechanisms, one on the virgin carbon surface and one involving metals, govern the removal process. Considering the difference in the redox capability of metals, each one of them should be considered separately. In fact assuming that nitrates would be the main products of surface reactions [12,26], the high capacity obtained on the sodium sample was apparently surprising since, taking into account the valency of metals, one would expect three times less NO_2 consumed than in the case of lanthanum and cerium. Analyzing the behavior of sodium chloride-NO_2 system, its ability to form nitrosyl chloride in the following reaction should be considered [45-47]:

$$2NO_2(g) + NaCl \rightarrow NaNO_3(s) + NOCl(g) \quad (10)$$

Extensive studies of this reaction showed that in the presence of water its rate is significantly enhanced. Moreover, in the reaction with HNO_3 sodium nitrate and HCl can be formed. Presence of nitric acid leads to the removal of chloride from the system [45]:

$$HNO_3 + 3HCl \rightarrow Cl_2 + 2H_2O + NOCl(g) \quad (11)$$

Thus even though nitrogen is possibly released from the system as nitrosyl chloride it cannot be detected by our sensor. The decrease in the concentration of NO_2 likely happens when nitric acid is present in excess after the reaction with carbon active centers and then it gets involved in reaction with sodium and HCl. If we assume that the carbon matrix surface has the same activity as that of the virgin carbon, about 6 mmol of NO_2 converted per 1 mmol of sodium indicates the catalytic effect and/or chain reaction related to formation of nitrosyl chloride. Moreover, release of CO_2 in reactions (4) and (6) and formation of carbonic acid in the presence of water can trigger formation of sodium carbonate. That carbonate is water-soluble thus can be removed by washing.

In the case of cerium different scenario is likely to occur. It is possible that first cerium(III) is oxidized by NO_2 to cerium(IV) and NO is formed. Than, when the reaction proceeds and nitric acid is formed on the carbon surface, that cerium(IV) reacts with it leading to $Ce(NO_3)_4$. Thus each cerium atom can engage four molecules of NO_2. Indeed if we compared the amount adsorbed to that on the virgin carbon the excess of 3.3 mmoles of NO_2 is retained. Taking into account that we have 0.7 mmoles of Ce(III) and assuming conversion to Ce(IV), 2.8 mmoles of NO_2 could be engaged in this reaction. The unaccounted NO_2 could be used for oxidation of Ce(III). Chlorine can be removed from the surface following reaction (10). That

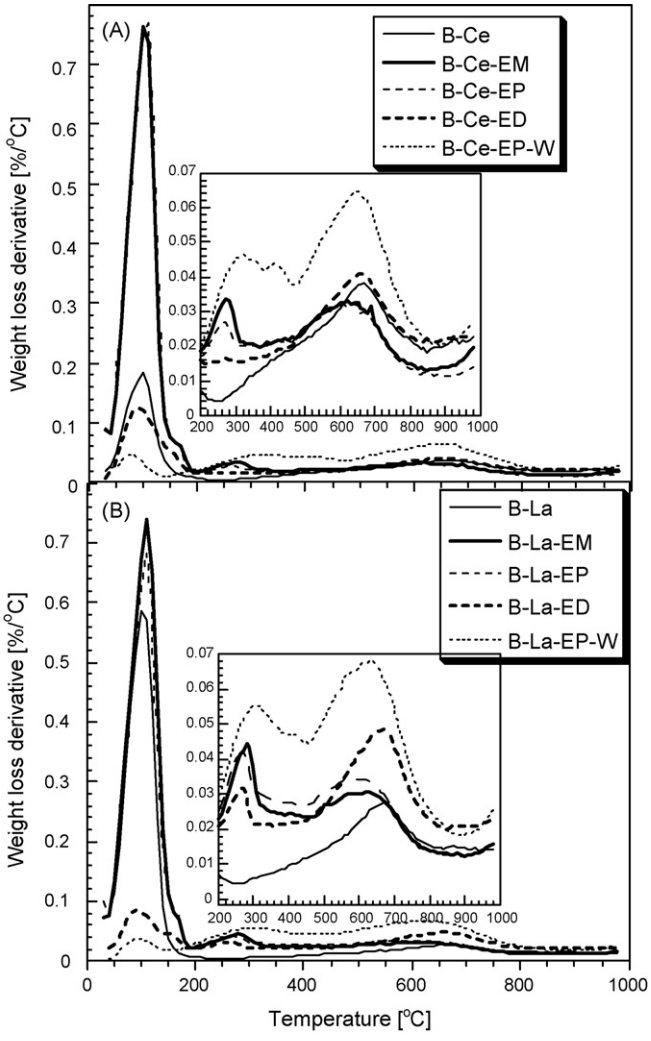

Fig. 8. DTG curves for B-Ce (A) and B-La (B) series of carbons.

Ce(IV) nitrate can also further oxidize the carbon surface which results in the strongest effect of cerium on the carbon matrix acidity.

In the case of lanthanum no additional NO_2 reduction is expected, besides that one taking place on the virgin carbon surface. Formation of lanthanum nitrates should engage the excess of NO_2 retained on the surface of this carbon compared to the virgin material. Since here only 1.2 mmoles of NO_2 is adsorbed per 1 mmol of La not full reaction capacity of La(III) is used. To explain this, and considering that the surface this carbon could not be washed with water, the formation of insoluble lanthanum species, possibly forms of carbonates, can be hypothesized. This is supported by FTIR and potentiometric titration results.

4. Conclusions

The results presented in this paper show an increase in the reactivity of carbons towards immobilization of nitrogen dioxide upon introduction of sodium, cerium and lanthanum chlorides. On their surface both carbonaceous matrix and inorganic phases are active. The latter is involved in the reduction of NO_2 to NO leading to incorporation of oxygen functional groups and $–NO_2$ to the graphene layers resulting in an increase in surface acidity. Presence of water enhances this process via formation of nitrous and nitric acids. When chlorides were present the capacity to interact with nitrogen dioxide increases since the inorganic phase, depending on the nature of metal, binds NO_2 in the forms of nitrates (Ce, La, Na), got oxidized/oxidized carbon surface (for Ce) or contributes to the formation of nitrosyl chloride (for Na). It was proposed that c erium(III) gets oxidized by NO_2, binds nitrogen as $Ce(NO_3)_4$ and then further oxidizes the carbon surface. On the other hand, NaCl interactions with NO_2 likely result in formation of nitrates and nitrosyl chloride. It is possible that some chain processes are involved here. Lanthanum, is the least efficient since besides forming nitrates there is an indication that it binds CO_2, formed as a result of carbon matrix oxidation by NO_2, as carbonates. This limits its ability to form nitrates.

Acknowledgement

This work was supported by ARO grant W911NF-05-1-0537.

References

[1] S.E. Manahan, Environmental Chemistry, 7th ed., CRC Press LLC, 2000, pp. 405–430.
[2] Y.W. Lee, H.J. Kim, J.W. Park, B.U. Choi, D.K. Choi, J.W. Park, Adsorption and reaction behavior for the simultaneous adsorption of NO–NO_2 and SO_2 on activated carbon impregnated with KOH, Carbon 41 (2003) 1881–1888.
[3] N. Shirahama, S.H. Moon, K.H. Choi, T. Enjoji, S. Kawano, Y. Korai, et al., Mechanistic study on adsorption and reduction of NO_2 over activated carbon fibers, Carbon 40 (2002) 2605–2611.
[4] B. Azambre, S. Collura, M.J. Trichard, J.V. Weber, Nature and thermal stability of adsorbed intermediates formed during the reaction of diesel soot with nitrogen dioxide, Appl. Surf. Sci. 253 (2006) 2296–2303.
[5] H. Muckenhuber, H. Hinrich, A DRIFTS study of the heterogeneous reaction of NO_2 with carbonaceous materials at elevated temperature, Carbon 45 (2007) 321–329.
[6] M. Jeguirim, V. Tschamber, J.F. Brilhac, P. Ehrburger, Interaction mechanism of NO_2 with carbon black: effect of surface oxygen complexes, J. Anal. Appl. Pyrol. 72 (2004) 171–181.
[7] Y. Kong, C.Y. Cha, NO_x adsorption on char in presence of oxygen and moisture, Carbon 34 (1996) 1027–1033.
[8] M.D. Ellison, M.J. Crotty, D. Koh, R.L. Spray, K.E. Tate, Adsorption of NH_3 and NO_2 on single-walled carbon nanotubes, J. Phys. Chem. B 108 (2004) 7938–7943.
[9] A.M. Rubel, J.M. Stencel, Effect of pressure on NO_x adsorption by activated carbons, Energy Fuels 10 (1996) 704–708.
[10] M.J. Illán-Gómez, A. Linares-Solano, L.R. Radovic, C. Salinas-Martínez de Lecea, NO reduction by activated carbons. 7. Some mechanistic aspects of uncatalyzed and catalyzed reaction, Energy Fuels 10 (1996) 158–168.
[11] W. Klose, S. Rincón, Adsorption and reaction of NO on activated carbon in the presence of oxygen and water vapour, Fuel 86 (2007) 203–209.
[12] R. Pietrzak, T.J. Bandosz, Activated carbons modified with sewage sludge derived phase and their application in the process of NO_2 removal, Carbon 13 (2007) 2537–2546.
[13] Y.W. Lee, J.W. Park, J.S.J. Jun, D.K. Choi, J.E. Yie, NO_x adsorption temperature programmed desorption and surface molecular ions distribution by activated carbon with chemical modification, Carbon 42 (2004) 59–69.
[14] A. García-García, M.J. Illán-Gómez, A. Linares-Solano, C. Salinas-Martínez de Lecea C, NO_x reduction by potassium-containing coal briquettes. Effect of preparation procedure and potassium content, Energy Fuels 16 (2002) 569–574.
[15] S. Matzner, H.P. Boehm, Influence of nitrogen doping on the adsorption and reduction of nitric oxide by activated carbons, Carbon 36 (1998) 1697–1709.
[16] P. Davini, SO_2 and NO_x adsorption properties of activated carbons obtained from a pitch containing iron derivatives, Carbon 39 (2001) 2173–2179.
[17] T.J. Bandosz, C.O. Ania, Surface chemistry of activated carbons and its characterization, in: T.J. Bandosz (Ed.), Activated Carbon Surfaces in Environmental Remediation. Interface Science and Technology, Vol. 7, Elsevier, 2006, pp. 159–229.
[18] L.R. Radovic, C. Sudhakar, Carbon as catalyst support: introduction, properties and applications, in: H. Marsh, E.A. Heintz, F. Rodriquez-Reinoso (Eds.), Introduction to Carbon Technologies, University of Alicante, Alicante, Spain, 1997, pp. 103–133.
[19] H. Jankowska, A. Swiatkowski, J. Choma, J. Active Carbon, Ellis Horwood, Poland, 1991.
[20] M.J. Illán-Gómez, S. Brandán, C. Salinas-Martínez de Lecea, A. Linares-Solano, Improvements in NO_x reduction by carbon using bimetallic catalysts, Fuel 80 (2001) 2001–2005.
[21] Y.W. Lee, J.W. Park, J.H. Yun, J.H. Lee, D.K. Choi, Studies on the surface chemistry based on competitive adsorption of NO_x–SO_2 onto a KOH impregnated activated carbon in excess O_2, Environ. Sci. Technol. 36 (2002) 4928–4935.
[22] Y.W. Lee, D.K. Choi, J.W. Park, Surface chemical characterization using AES/SAM and ToF-SIMS on KOH-impregnated activated carbon by selective adsorption of NO_x, Ind. Eng. Chem. Res. 40 (2001) 3337–3345.
[23] B.J. Oark, S.J. Park, S.K. Ryu, Removal of NO over copper supported on activated carbon prepared by electroless plating, J. Coll. Interf. Sci. 217 (1999) 142–145.
[24] H. Yamashita, A. Tomita, Influence of char surface chemistry on the reduction of nitric oxide with chars, Energy Fuels 7 (1993) 85–89.
[25] M.J. Illán-Gómez, A. Linares-Solano, L.R. Radovic, C. Salinas-Martínez de Lecea, NO reduction by activated carbons. 2. Catalytic effect of potassium, Energy Fuels 9 (1995) 97–103.
[26] G.M. Underwood, T.M. Miller, V.H. Grassian, Transmission FT-IR and Knudsen cell study of the heterogeneous reactivity of gaseous nitrogen dioxide on mineral oxide particles, J. Phys. Chem. A 103 (1999) 6184–6190.
[27] J.T. Richardson, Principles of Catalyst Development, Plenum press, New York, 1989, p. 95.
[28] T.J. Bandosz, A. Bagreev, F. Adib, A. Turk, Unmodified versus caustics impregnated carbons for control of hydrogen sulfide emissions from sewage plants, Environ. Sci. Technol. 34 (2000) 1069–1074.
[29] J. Jagiello, Stable numerical solution of the adsorption integral equation using splines, Langmuir 10 (1994) 2778–2785.
[30] J. Jagiello, T.J. Bandosz, J.A. Schwarz, Carbon surface characterization in terms of its acidity constant distribution, Carbon 32 (1994) 1026–1028.
[31] M.M. Dubinin, in: P.L. Walker (Ed.), Chemistry and Physics of Carbon, Vol. 2, Dekker, New York, 1966, pp. 51–120.
[32] J.P. Olivier, Modeling physical adsorption on porous and nonporous solids using density functional theory, J. Porous Mater. 2 (1995) 376–377.
[33] C.M. Lastoskie, K.E. Gubbins, N. Quirke, Pore size distribution analysis of microporous carbons: a density functional theory approach, J. Phys. Chem. 97 (1993) 4786–4796.
[34] M. Jequirim, V. Tschamber, J.F. Brilhac, P. Ehrburger, Oxidation mechanism of carbon black by NO_2: effect of water vapour, Fuel 84 (2005) 1949–1956.
[35] J. Szanyi, J.H. Kwak, R.J. Chimentao, C.H.F. Peden, Effect of H_2O on the adsorption of NO_2 on γ-Al_2O_3: an in situ FTIR/MS study, J. Phys. Chem. C 111 (2007) 2661–2669.
[36] P.K. Hudson, J. Schwarz, J. Baltrusaitis, E.R. Gibson, V.H. Grassian, A spectroscopic study of atmospherically relevant concentrated aqueous nitrate solutions, J. Phys. Chem. A111 (2007) 544–548.
[37] K. Hadjiivanov, V. Avreyska, D. Klissurski, T. Marinova, Surface species formed after NO adsorption and NO + O_2 coadsorption on ZrO_2 and sulfated ZrO_2: an FTIR spectroscopic study, Langmuir 18 (2002) 1619–1625.
[38] J. Zawadzki, M.W. Wisniewski, K. Skowronska, Heterogenous reactions of NO_2 and NO–O_2 on the surface of carbons, Carbon 41 (2003) 235–246.
[39] R.C. Weast, Handbook of Chemistry and Physics, 62nd ed., CRC Press, Boca Raton, FL, 1981, pp. 73–166 (Section B).
[40] I.I. Salame, T.J. Bandosz, Comparison of the surface features of two wood-based activated carbons, Ind. Eng. Chem. Res. 39 (2000) 301–306.
[41] E. Papirer, J. Dentzer, S. Li, J.B. Donnet, Surface groups on nitric acid oxidized carbon black samples determined by chemical and thermodesorption analyses, Carbon 29 (1991) 69–72.
[42] H. Muckenhuber, H. Grothe, The heterogeneous reaction between soot and NO_2 at elevated temperature, Carbon 44 (2006) 546–559.
[43] G. Ghingo, M. Causa, A. Maranzana, G. Tonachini, Aromatic hydrocarbon nitration under troposperic and combustion conditions. A theoretical mechanistic study, J. Phys. Chem. 110 (2006) 13270–13282.

[44] A.J. Fletcher, Y. Yüzak, K.M. Thomas, Adsorption and desorption kinetics for hydrophilic and hydrophobic vapors on activated carbon, Carbon 44 (2006) 989–1004.
[45] H. Yoshitake, Effects of surface water on NO_2–NaCl reactions studied by diffuse reflectance infrared spectroscopy (DRIFT), Atmos. Environ. 34 (2000) 2571–2580.
[46] W.H. Schroeder, P. Urone, Formation of nitrosyl chloride from salt Particles in air, Environ. Sci. Technol. 8 (1974) 756–758.
[47] J.K.S. Wan, J.N. Pitts Jr., P. Beichert, B.J. Finlayson-Pitts, The formation of free radical Intermediates in the reactions of gaseous NO_2 with slid NaCl and Na–Br—atmospheric and toxicological implications, Atmos. Environ. 30 (1996) 3109–3113.